Supplemental information

Figure legends

Fig. S1. Structure/localization analysis of Yps oocyte targeting.

The distributions of full-length and truncated Yps proteins are shown. Red, Yps; Green, F-actin; Blue, TOPRO3. Full length Yps (YpsF; 1-352 a.a.; A-C), the N-terminal half (YpsN; 1-160 a.a.; D-F), the C-terminal half (YpsC; 161-352 a.a.; G-I), and full length lacking the CSP (cold shock protein) domain (YpsΔCSP; 1-62 a.a. and 132-352 a.a.; J-L) were subcloned into the vector pDONOR201 using the Gateway system (Invitrogen), and transferred to the pUASp vector (pPWR) containing mRFP at the C-terminus region. Maternal triple GAL4 drivers were used to express the transgenes in the germline. YpsF and YpsN were enriched in the oocyte at stage 6 (yellow boxes in B and E) and the posterior pole at stage 10 (yellow arrows in C and F). YpsN contains and Exu binding site and a putative RNA binding site (Wilhelm et al., 2000). In contrast, YpsC and YpsΔCSP were localized to nuclei in egg chambers (green arrows in H and K). These results indicate that the CSP domain is necessary for Yps localization to the oocyte. Bars: (A, B, D, E, G, H, J, and K) 10 μm; (C, F, I, and L) 50 μm.

Fig. S2. Fluorescence loss in photobleach (FLIP) analysis in young egg chambers.

FLIP analysis was performed with stage-6 egg chambers expressing *Dendra2* (a and b) and *GFP::Yps* (c and d). Representative images after each photobleach are shown. As the relative positions of the oocyte and four adjoining nurse cells are different with individual egg chambers, we took Z optical sections of images before photobleaching and found cases in which the oocyte and a nurse cell are not overlapping along the Z-axis. We also chose egg

chambers in which the oocyte is located closest to the objective lens. Membranes were labeled with FM4-64 to visualize cell-cell boundaries. For photobleaching, we set the region of interest (ROI) and enlarged the pinhole to cover the entire cell volume. Areas of photobleach are outlined with yellow lines. We scanned the ROI with a 488nm laser at the maximal level (100%). A single-plane image was recorded after photobleaching 5 times at 3-minute intervals (blue arrows). Loss of fluorescence in cells neighboring the bleached cell indicates proteins can move through ring canals and become photobleached in the region of interest. Note that the amount of fluorescence loss was greater in the neighboring cells to ROI compared to a nurse cell at the anterior of the egg chamber. Bar, 10 μm.

Fig. S3. Endogenous Yps responds to nutrient stress as do GFP::Yps or YpsN::mRFP Stage-6 egg chambers were dissected from females reared on protein-rich (A-C, G-I, M, and N) or protein-poor food for 48 hrs (D-F, J-L, O, and P), and then immunostained with anti-Yps antibody. While most GFP::Yps or YpsN::mRFP aggregates were detected with anti-Yps antibody (yellow arrows in A-L), some YpsN::mRFP aggregates contained less endogenous Yps, suggesting that overexpressed products made aggregates more readily in response to nutrient stress (blue arrows in J-L). Endogenous Yps made aggregates in the wild-type background, although the number of particles was less than that of GFP::Yps (arrows in M-P). Genotype: (A-F) *GFP::Yps,* (G-L) *matalpha4-GAL-VP16/YpsN::mRFP,* (M-P) *yw*. Note that endogenous Yps was less detected at the centers of egg chambers, because antibodies did not penetrate well into the tissue. Bars, 20 μm.

Fig. S4. The distribution of *oskarMS2*/MS2-GFP is affected by protein deprivation. Female flies expressing *oskarMS2/MS2-GFP* were placed on protein-rich food with yeast or

protein-poor food for 24 hrs. Their ovaries were dissected and incubated in Schneider's *Drosophila* medium (SDM) containing FM4-64. In the protein-rich condition, *oskarMS2*/MS2-GFP was exclusively enriched in the oocyte at stage 6 (A), stage 7 (C), and stage 8 (E), and localized to the posterior pole at stage 9 (G). In the protein-poor condition, *oskarMS2*/MS2-GFP accumulated in nurse cells at stage 6 (B), stage 7 (D), and stage 8 (F) as indicated by arrows. Starved egg chambers degenerated by apoptosis after stage 8. Bar, 10 μm.

Fig. S5. Yps particles colocalized with processing body markers, but not with stress granule or autolysosome markers.

(A-E) Stage-6 egg chambers from 48 hr-starved females expressing *GFP::Yps* were immunostained with antibodies against Decapping protein 1 (Dcp1, A), the 5´-3´ exoribonuclease Pacman (Pcm, B), eukaryotic initiation factor 4E (eIF4E, C), Staufen (Stau, D), and phosphorylated eIF2α (E). GFP::Yps was mostly colocalized with Dcp1 (68.8 %, n = 378 particles/23 egg chambers), Pcm (70.7 %, n = 232 particles/12 egg chambers), and eIF4E (92.5 %, n = 212 particles/8 egg chambers), but not with Stau (0.3 %, n = 59 particles/13 egg chambers). (F) Stage-6 egg chambers were dissected and immediately treated with an acidotropic dye LysoTracker (red) for 5 min in SDM. LysoTracker hardly colocalized with GFP::Yps aggregates after 24 hrs of starvation (0.58 %, n = 1214 particles/24 egg chambers). In all images, GFP::Yps is green. White boxes in the left column are 10 μm-wide squares and magnified in the right columns.

Movie Legends

Movie S1. Yps-containing particles move toward the oocyte along microtubules (MTs) during stage 6.

A stage-6 egg chamber expressing *YpsN::mRFP* and *GFP::tubulin* under the control of germline GAL4 drivers. Note that some YpsN::mRFP particles (magenta) move toward the oocyte along polarized MTs extending through the ring canal between nurse cells and the oocyte. Images were taken at 5-second intervals. Bar, 10 μm.

Movie S2. GFP::Yps moved out of the oocyte after colchicine treatment.

A stage-6 egg chamber expressing *GFP::Yps* was incubated in SDM with 50 μg/ml colchicine for 1 hr. Membranes were labeled with FM4-64. Images were taken at the interval of 15 seconds for 50 minutes in total. GFP::Yps aggregates are detected both in nurse cells and the oocyte. Note that GFP::Yps signals move out of the oocyte when MT organization is disrupted.

Movie S3. 3-D analysis of GFP::Yps aggregates in a stage-8 egg chamber from a starved female.

Z sections of a stage-8 egg chamber were reconstructed by Imaris (Bitplane). GFP::Yps aggregates were labeled with pink-color surfaces.

Movie S4. The dynamic property of Yps aggregates in a stage-6 egg chamber from a starved female.

Female flies were deprived of protein for 4 hrs and dissected. In response to starvation,

YpsN::mRFP particles continuously assembled and disassembled in nurse cell cytoplasm (white box), showing the dynamic property of Yps aggregates. Above the white inset, a pair of the black spots indicates a ring canal between a nurse cell and the oocyte. The black area in the left is a nurse cell nucleus. Images were taken at 18-second intervals. Bar, 10 μm.

Movie S5. The dynamic movement of EB1::GFP in well-fed females.

Female flies expressing *EB1::GFP* were reared on protein-rich food for 2 days and dissected. In a stage-6 egg chamber, many EB1::GFP comets are visible in the oocyte and nurse cells, revealing active polymerization of MT. Images were taken at 5-second intervals. Bar, 10 μm.

Movie S6. The movement of EB1::GFP was detected in the cortical region of nurse cells from starved females.

Female flies expressing *EB1::GFP* were deprived of protein-rich food for 3 days and dissected. EB1::GFP comets still visible throughout cytoplasm, indicating that MT polymerization still occurs under the protein-poor condition. However, EB1::GFP comets appeared to move more slowly than in egg chambers from well-fed females, and fluorescence was more stable in the cortical regions of the oocyte and nurse cells. These observations suggest that the response to poor nutrition includes an alteration of MT polymerization rates, especially in near plasma membranes. Images were taken at 5-second intervals. Bar, 10 μm.

Table S1. The distributions of cytoplasmic proteins in stage 6-7 egg chambers.

	Functional Category	*Protein*	*CG*	*Molecular Function*
Oocyte Enriched	RNA binding	Bel	CG9748	nucleic acid binding, helicase
		eIF-4E	CG4035	mRNA cap binding
		Growl	CG14648	RNA binding
		Imp	CG1691	mRNA binding
		Shep	CG32423	mRNA binding
		Sqd	CG16901	mRNA binding
		Yps	CG5654	mRNA binding
	ER/Golgi	Fkbp13	CG9847	peptidyl-prolyl isomerase
		l(1)G0320	CG32701	SRP binding
		Pdi	CG6988	protein disulfide isomerase
		Rtnl1	CG33113	receptor signaling protein
		Sec61alpha	CG9539	protein transporter
		Tral	CG10686	ER to Golgi transport
	Signaling	Cam	CG8472	calcium binding
		Sdc	CG10497	transmembrane receptor
		Sag	CG2621	Kinase
	Metabolism	CG12163	CG12163	cysteine-type endopeptidase
		Vha16	CG3161	proton pump subunit
	Unknown	Bsg	CG31605	
Ubiquitous	Protein synthesis/folding	CG8443	CG8443	translation initiation factor
		CG10990	CG10990	translation elongation factor
		Elf	CG6382	translation release factor
		eRF1	CG5605	translation release factor
		Hsc70Cb	CG6603	chaperone binding
		RpL30	CG10652	ribosome protein
		Sop (RpS2)	CG5920	ribosome protein
		Tpr2	CG4599	heat shock protein binding
	Metabolism	Argk	CG32031	arginine kinase
		CG6084	CG6084	aldehyde reductase activity
		CG6783	CG6783	fatty acid binding
		CG8036	CG8036	transketolase activity
		CG31694	CG31694	hydrolase, receptor binding
		CG32549	CG32549	5'-nucleotidase activity
		Fer1HCH	CG2216	iron binding
		Oda	CG16747	ornithine decarboxylase antizyme
		Sh3ß	CG8582	metal ion binding, copper
		Trxr-1	CG2151	glutathione-disulfide reductase
		VhaSFD	CG17332	proton pump subunit
	Cytoskeleton	ßTub56D	CG9277	GTPase
		Lasp	CG3849	actin binding
		Jupiter	CG31363	microtubule binding
		Tsr	CG4254	actin binding
	Signaling	14-3-3ε	CG31196	SUMO binding

		Btk29A	CG8049	tyrosine kinase
	Unknown	CG1104	CG1104	
		CG15926	CG15926	
		Fax	CG4609	
		Larp	CG42551	

The protein trap screen allowed us to obtain a lot of transgenic lines that show specific GFP localization patterns in egg chambers. Among 48 genes that were expressed in germline cytoplasm, 19 showed GFP signals enriched in the oocyte, while 29 were ubiquitously distributed in the cytoplasm. When we compared a group of proteins that is enriched or not enriched in the oocyte, they could be classified into several functional groups. The oocyte-enriched proteins included most RNA binding proteins and all endoplasmic reticulum (ER) proteins in our collection. Most RNA binding proteins were enriched in the oocyte starting during stage 2, while the localization of ER proteins became prominent during stage 6. On the other hand, ribosomal proteins, protein synthesizing factors, or metabolic proteins were ubiquitously distributed. This result suggests that there is an active sorting mechanism between nurse cells and oocyte based on their cellular functions.

Table S2. The developmental stage of previtellogenic egg chambers in our analysis

Stage	egg chamber (n)	Major axis length (μm)	Minor axis width (μm)	Oocyte area (μm^2)	Whole area of egg chamber (μm^2)	Nurse cell nucleus Diameter (μm)
3	24	41.0±0.8 (SEM)	38.0±0.9	97.0±4.0	1180.5±46.3	7.9 ± 0.2
4	33	54.1±1.1	47.1±0.8	127.6±4.3	1912.3±65.9	10.7 ± 0.2
5	42	76.3±1.7	59.3±1.0	211.6±8.7	3399.3±124.2	14.6 ± 0.4
6	37	91.4±1.3	66.7±0.8	290.0±10.3	4576.1±110.3	16.5 ± 0.4
7	30	115.4±3.5	71.2±1.4	450.8±26.6	6096.9±291.5	20.4 ± 0.5
8	20	158.3±3.3	87.4±1.6	790.5±43.9	9884.0±394.4	25.8 ± 0.6

As previtellogenic stages are difficult to distinguish in living egg chambers, we measured the size of egg chambers to determine their stages. The length, the width, the whole area, the oocyte area of egg chamber, and the diameter of nurse cell nuclei were measured with LSM510-attached software. For the image analysis, a single focal plane was selected in which the area of whole egg chamber or the oocyte is maximized. In addition to the sizes, there are several features of previtellogenic stages as described previously (Lin and Spradling, 1993; Spradling, 1993); stage 1 is the last part of germarium; stage 2 to 6 can be relatively distinguished in the context of an entire ovariole; the oocyte nucleus is located at the posterior at stage 7; Yolk deposition starts at stage 8. The stage in our analysis is identical to the previous reports.

References

Lin, H., Spradling, A. C., 1993. Germline stem cell division and egg chamber development in transplanted Drosophila germaria. Dev Biol. 159**,** 140-52.

Spradling, A. C., 1993. The developmental genetics of oogenesis. Cold Spring Harbor Laboratory Press, Plainview, N.Y.

Wilhelm, J. E., Mansfield, J., Hom-Booher, N., Wang, S., Turck, C. W., Hazelrigg, T., Vale, R. D., 2000. Isolation of a ribonucleoprotein complex involved in mRNA localization in Drosophila oocytes. J Cell Biol. 148**,** 427-40.

Shimada et al.
Figure S1

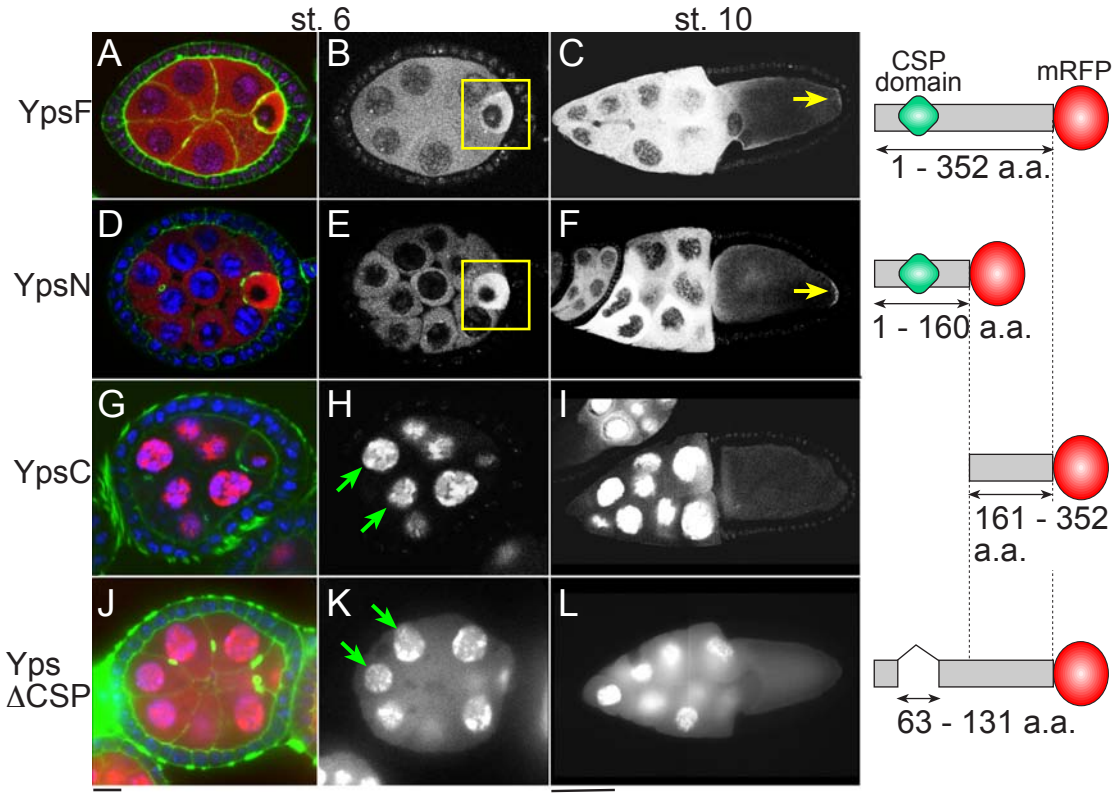

Shimada et al.
Figure S2

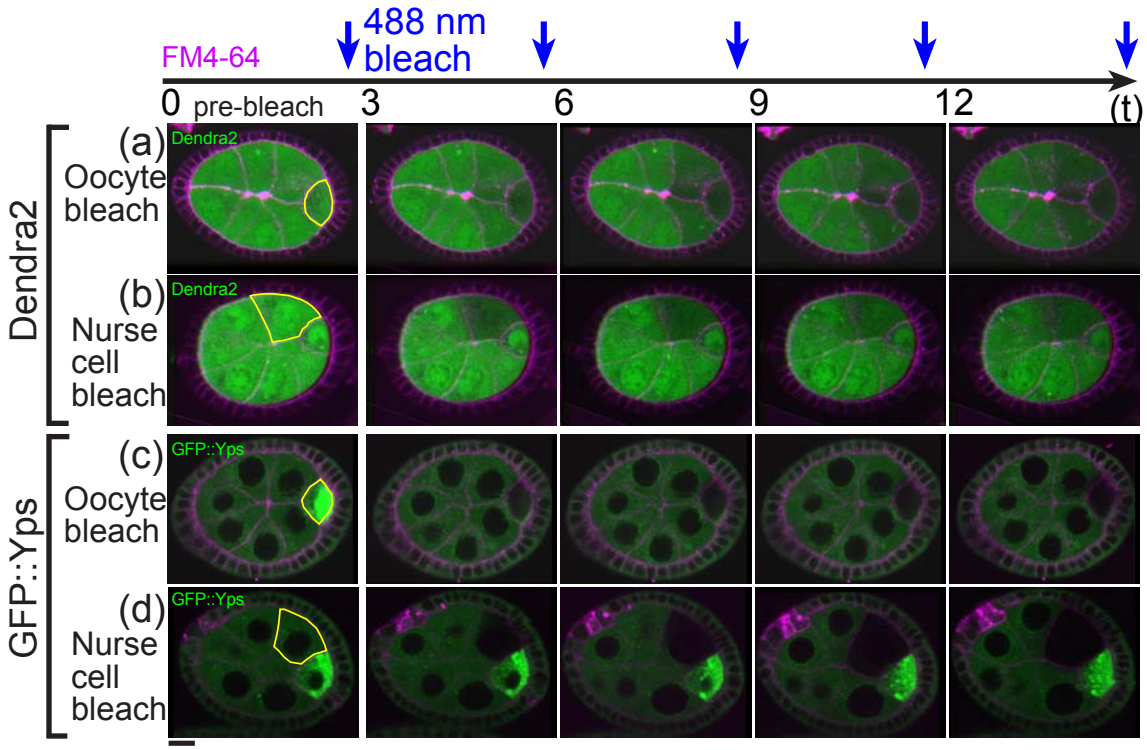

Shimada et al.
Figure S3

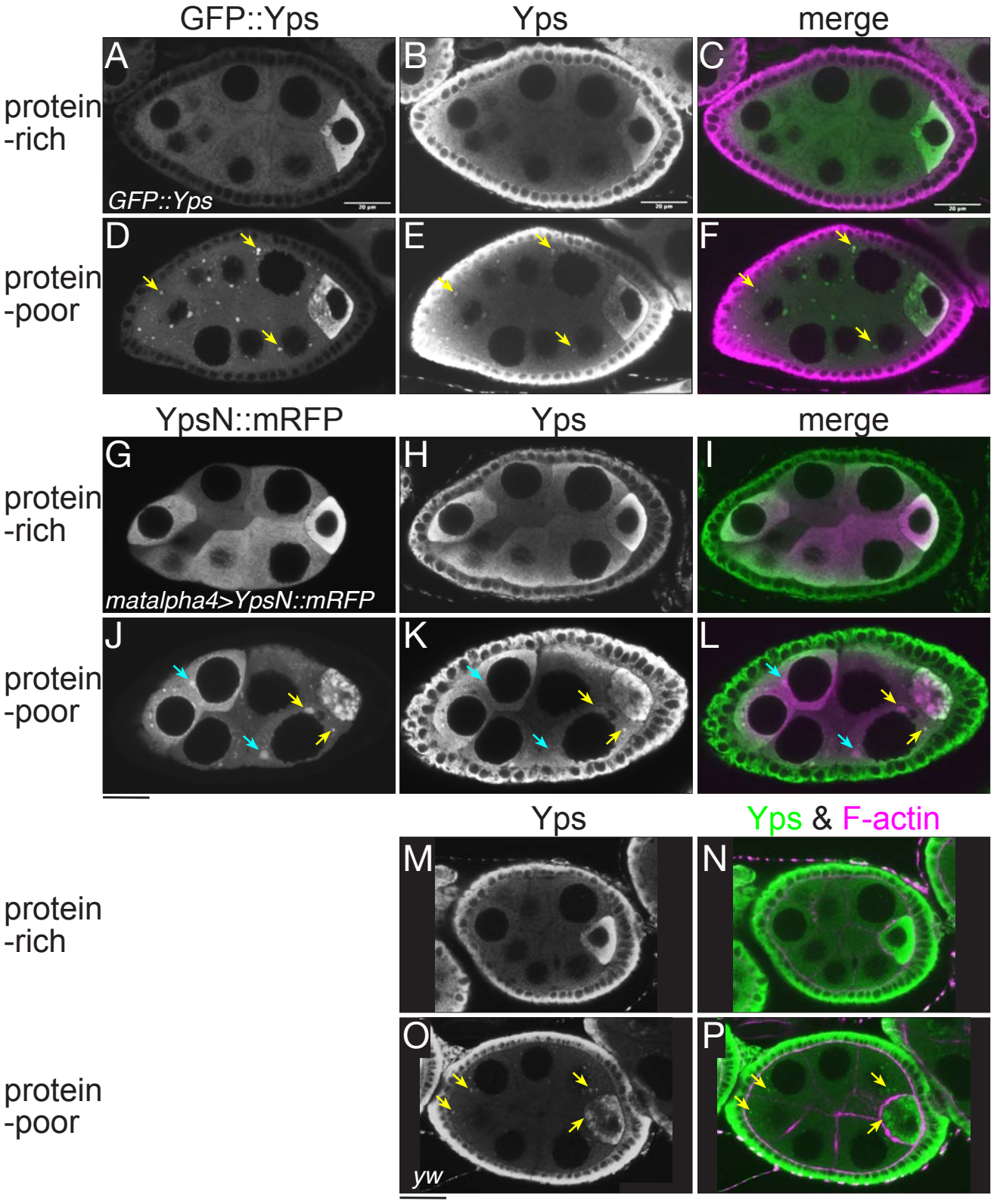

Shimada et al.
Figure S4

oskMS2/MS2-GFP
FM4-64

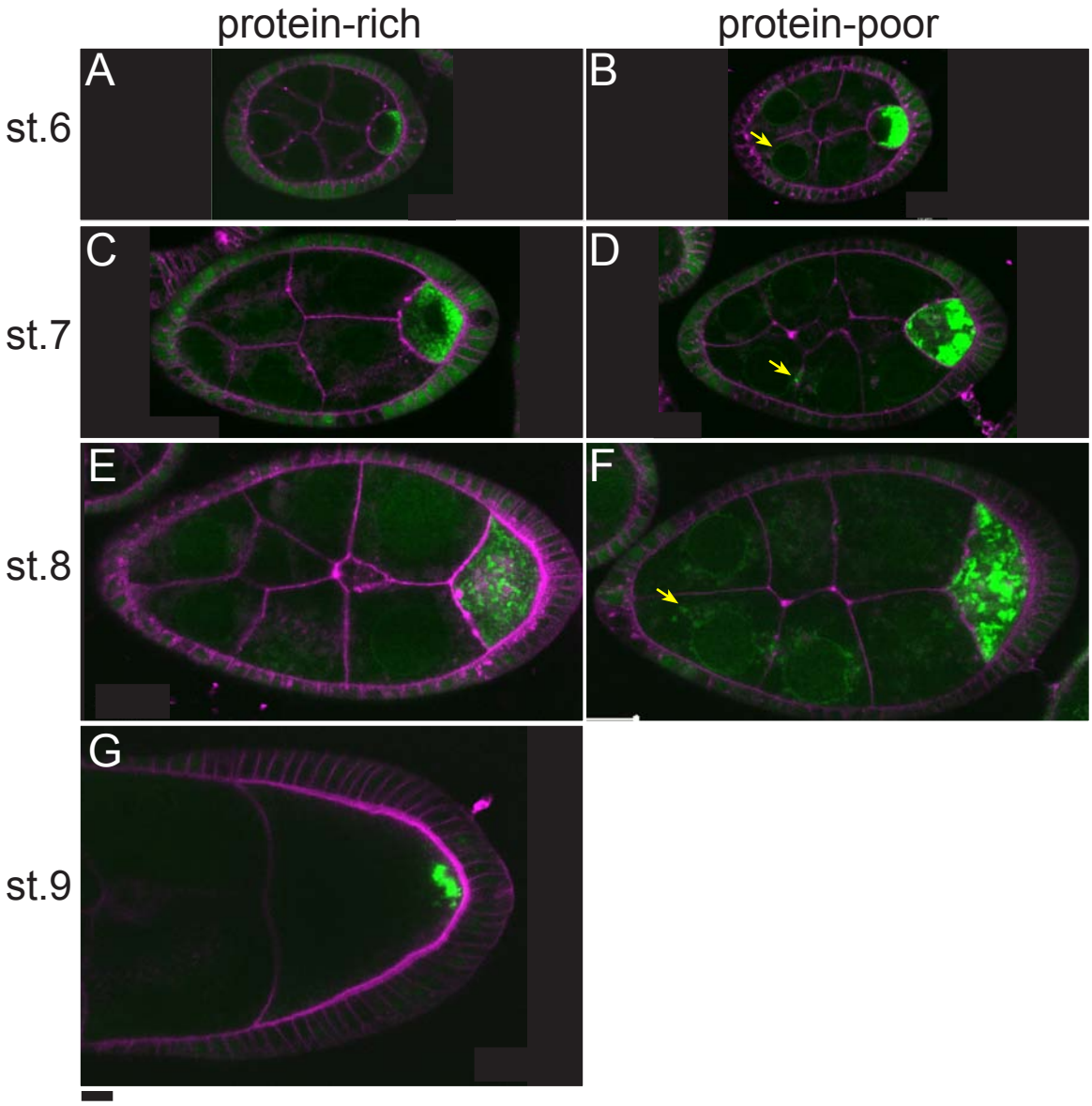

Shimada et al.
Figure S5